



## MONITORING POTENTIAL IONOSPHERE CHANGES CAUSED BY VAN EARTHQUAKE (Mw 7.2) USING GNSS MEASUREMENTS

Selcuk PEKER<sup>1</sup>, Samed INYURT<sup>2</sup> and Cetin MEKIK<sup>2</sup>

<sup>1</sup>General Command of Mapping, Ankara, Turkey

<sup>2</sup>Bulent Ecevit University, Geomatics Engineering Department, Zonguldak

### ABSTRACT

Several scientists from different disciplines have studied earthquakes for many years. As a result of these studies, it has been proposed that some changes take place in the ionosphere layer before, during or after earthquakes, and the ionosphere should be monitored in earthquake prediction studies. This study investigates the changes in the ionosphere created by the earthquake with magnitude of Mw=7.2 in the northwest of the Lake Erçek which is located to the north of the province of Van in Turkey on 23 October 2011 and at 1.41 pm local time (-3 UT) with the epicenter of 38.758° N, 43.360° E using the TEC values obtained by the Global Ionosphere Models (GIM) created by IONOLAB-TEC and CODE. In order to see whether the ionospheric changes obtained by the study in question were caused by the earthquake or not, the ionospheric conditions were studied by utilizing indices providing information on solar and geomagnetic activities (F10.7 cm, Kp, Dst).

As a result of the statistical test on the TEC values obtained from the both models, positive and negative anomalies were obtained for the times before, on the day of and after the earthquake, and the reasons for these anomalies are discussed in detail in the last section of the study. As the ionospheric conditions in the analyzed days were highly vibrant, it was thought that the anomalies were caused by geomagnetic effects, solar activity and the earthquake. The authors believe that interdisciplinary studies are needed to distinguish the earthquake-related part of the anomalies in question.

**Keywords:** TEC, Van Earthquake, Ionosphere



## 1. INTRODUCTION

The ionosphere is the part of the atmosphere at the altitudes of 60 km to 1.100 km where there are ions and free electrons in considerable amounts that can reflect electromagnetic waves (URL-1). It completely covers the thermosphere, one of the main layers of the atmosphere, but also includes some of the mesosphere and the exosphere.

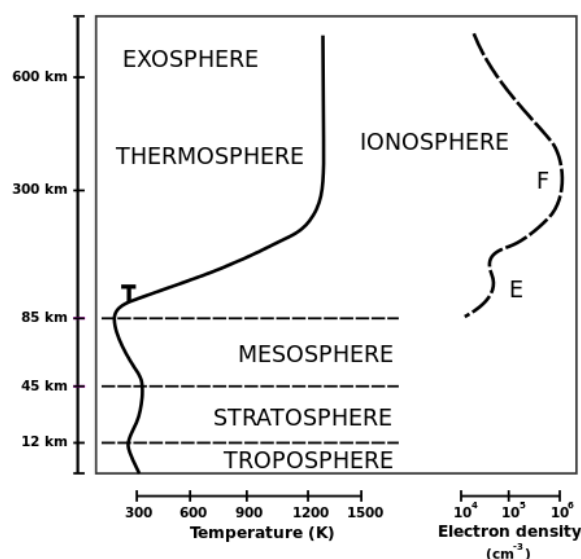


**Figure 1.** The Relationship between the Atmosphere and the Ionosphere (URL-2)

The atmospheric gas molecules in the layer in question are charged with electricity influenced by the UV radiation from sunlight and disintegrating into ions and electrons, hence leading to ionization. As a result of this ionization, especially the fields of information and communication technologies, intensely using audio, data and signal interactions, are affected by the ionosphere (Anderson and Fuller-Rowell, 1999)

When a radio wave reaches the ionosphere, the electric component of the electromagnetic wave forces the electrons in the ionosphere to vibrate in the same frequency as the radio wave. The vibration energy leads to reorganization of the electrons or the electrons' replication of the original radio frequency. If the collision frequency of the ionosphere is lower than the radio frequency and the quantity of electrons is sufficient, complete reflection occurs. If the frequency



of the radio wave is higher than the plasma frequency of the ionosphere, electrons cannot provide feedback fast enough, and thus the signal is not reflected.

The most important parameter that defines the ionosphere in space and time is the quantity of electrons. This quantity varies under the influence of the day-night cycle, seasons, geographical location and magnetic storms in the sun. As it is not possible to measure the quantity of electrons in the ionosphere directly, indirect measurement and calculation methods have been developed. Total Electron Content (TEC), which is defined as the quantity of free electrons along a cylinder with a cross section of  $1 \text{ m}^2$ , is a suitable parameter to monitor the changes in the ionosphere in space and time. All signals that contain audio and data that pass through or get reflected from the ionosphere, which is highly irregular and difficult to model, are affected by the structure of this layer.

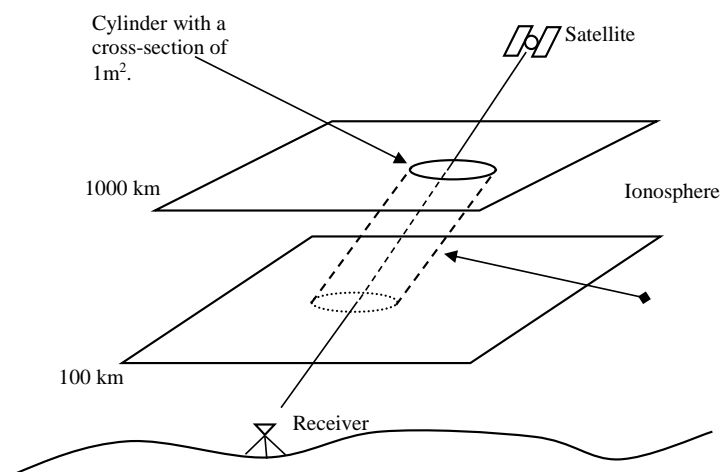


**Figure 2.** Graphical Representation of Total Electron Content (Langley, 2002)

Calculating Total Electron Content (TEC) is a method used directly to investigate the structure of the ionosphere. TEC is represented by the unit of TECU, and one TECU equals to  $10^{16} \text{ el/m}^2$  (Schaer, 1999). TEC is expressed in two ways: STEC (Slant Total Electron Content); the free electron content calculated along the slanted line between the receiver and the satellite, and VTEC (Vertical Total Electron Content); the free electron content calculated along the zenith of the receiver (Langley, 2002).



81 TEC varies based on positional and temporal variables such as the latitude of the place, seasons,  
 82 solar activity, geomagnetic storms and earthquakes. Ionospheric altitude also differs based on  
 83 geography.

84 TEC, which is defined as the number of free electrons on the one square meter area on the line  
 85 followed by a radio wave, is one of the important parameters for examining the structure of the  
 86 ionosphere and the upper atmosphere. With TEC values, it is possible to examine the short and  
 87 long-term changes in the ionosphere, ionospheric irregularities and disruptive factors together  
 88 (Erol and Arıkan 2005; Başpınar 2012).

89 The changes in the ionosphere created by earthquakes were first studied in early 1960s. In order  
 90 to detect any prior sign before earthquakes, experts examined the critical frequency, the  
 91 maximum electron density in the F2 layer and total electron content (Yildirim et al., 2016).  
 92 Some studies have shown that ionospheric anomalies may be detected in a short time before  
 93 earthquakes using satellites (Pulinets 1998).

94 Ionospheric changes are being studied in more than twenty countries today as precursors of  
 95 earthquakes. Definition of ionospheric anomalies and feasibility studies of sismo-ionospheric  
 96 precursors are still ongoing (Yildirim et al., 2016).

97

## 98 2. METHODOLOGY

99

### 100 2.1 IONOLAB-TEC Method:

101

102 The IONOLAB-TEC method developed by the department of Electrical and Electronics  
 103 Engineering of Hacettepe University is a JAVA application that uses the Regularized TEC (D-  
 104 TEI) algorithm (Arıkan et al. 2004 ).

105 In this application, they developed a method that estimates VTEC values by using all GPS  
 106 signals measured at a period of time in a day. While the measurements taken from the satellites  
 107 with elevations of  $60^\circ$  or higher are used, the measurements from the satellites with elevations  
 108 of  $10^\circ$  to  $60^\circ$  are weighted by a Gauss function. The data from satellites with elevations of  
 109 lower than  $10^\circ$  are not included in calculations to reduce multipath effects (Equations 1).

110

$$\begin{aligned}
 &111 \\
 &112 \quad \omega_m(n) \quad \left\{ \begin{array}{ll} 1, & 60^\circ \leq \epsilon_m(n) \leq 90^\circ \\ \exp(-(60 - \epsilon_m(n))^2 / 2\sigma^2), & 10^\circ \leq \epsilon_m(n) < 60^\circ \\ 0, & \epsilon_m(n) < 10^\circ \end{array} \right. \quad (1) \\
 &113
 \end{aligned}$$



114

115 In the next step, the VTEC data obtained from satellites are combined by the least squares  
 116 method. For this, a cost function that will minimize the square of the error between the VTEC  
 117 data that will be obtained as a result of estimation, and the VTEC data calculated from the  
 118 satellites is defined as below.

$$119 \quad J_{\mu, k_c}(x) = \sum_{m=1}^M (x - x_m)^2 W_m(x - x_m) + \mu x^T H(k_c) \quad (2)$$

$$120 \quad W_m = \text{diag}(w_m),$$

121  $H(k_c)$  = Filter that allows components of frequencies up to  $k_c$  to pass,

122  $\mu$  = Regularization coefficient.

123 To find the  $x$  estimates that minimize the error, if the derivative of the statement in Equation  
 124 (2) is taken and equated to 0;

$$125 \quad (\Delta_x J_{\mu, k_c}(x)) = 0 \quad (3)$$

126 The minimization process for the cost function turns into the solution of a linear system like:

$$127 \quad A(\mu, k_c)x = b \quad (4)$$

128 In the equation above:

$$129 \quad A(\mu, k_c) = \sum_{m=1}^M W_m + \mu H(k_c) \quad (5)$$

$$130 \quad b = \sum_{m=1}^M W_m x_m \quad (6)$$

131 Therefore, the VTEC estimates  $\tilde{\mathbf{x}}$  are found as,

$$132 \quad \tilde{X}(\mu, k_c) = A^{-1}(\mu, k_c)b \quad (7)$$

133 The high-pass penalty filter used for TEC estimates may be organized as the  $\mathbf{H}(k_c)$  Toeplitz  
 134 matrix:

$$135 \quad \mathbf{H}(k_c) = \begin{bmatrix} h_0(k_c) & h_1(k_c) \wedge & h_{N-1}(k_c) \\ h_{N-1}(k_c) & h_0(k_c) \wedge & h_{N-2}(k_c) \\ \vdots & \vdots & \vdots \\ h_1(k_c) & h_2(k_c) \wedge & h_0(k_c) \end{bmatrix} \quad (8)$$

136

$$137 \quad h_n(k_c) = \frac{1}{N} \sum_{k=0}^{N-1} H_k(\omega_c) \exp(j \frac{2\pi}{N} kn) \quad (9)$$

138  $\omega_c = 2\pi k_c / N$ . The filter function  $\mathbf{H}_k(\omega_c)$  may be chosen as in Equation (11).

$$139 \quad H_k(\omega_c) = \begin{cases} 1, & \text{if } \pi - \omega_c \leq \frac{2\pi}{N} k \leq \pi + \omega_c \\ 0, & \text{diger} \end{cases} \quad (10)$$



$$h_n(k_c) = \begin{cases} 1 - \frac{1}{N}(2k_c + 1), & n = 0 \\ -\sin\left(\frac{\pi n}{N}(2k_c + 1)\right) \left(N \sin\left(\frac{\pi n}{N}\right)\right), & n \neq 0 \end{cases} \quad (11)$$

The error function between the VTEC values calculated from satellites  $\mathbf{x}_m$  and the VTEC estimates  $\tilde{\mathbf{x}}$  is given in Equation (12). The operation  $\|\cdot\|$  describes the norm statement of the difference vector weighted between the VTEC estimates and calculations.

$$e(\mu, k_c) = \sum_{m=1}^M \|\mathbf{W}_m(\tilde{\mathbf{x}} - \mathbf{x}_m)\|^2 \quad (12)$$

In order to regularize the estimate values even more, floating median filter may be used. The length of the median filter is another parameter to be determined. With the estimated VTEC values, post-estimation median filter was applied, and the error function between the VTEC values is given in Equation (13).

$$e_f(N_f) = \|\tilde{\mathbf{x}} - \tilde{\mathbf{x}}_{N_f}\|^2 \quad (13)$$

In Equation (13),  $\tilde{\mathbf{x}}_{N_f}$  shows the  $\tilde{\mathbf{x}}$  estimates processed with a median filter with the length of  $N_f$ . For the method to work accurately, suitable  $\mu$ ,  $k_c$  and  $N_f$  parameters must be determined. The details provided up to now cover the regularization method for a period of 24 hours.

When there is an estimation of TEC for a limited period of time, the cost function is redefined as in Equation (14).

$$J_{\mu, k_c}(\mathbf{x}) = \sum_{m=1}^M (\mathbf{x} - \mathbf{x}_m)^T \mathbf{W}_m (\mathbf{x} - \mathbf{x}_m) + \mu (\mathbf{x} - \mathbf{a})^T \mathbf{H}(k_c) (\mathbf{x} - \mathbf{a}) \quad (14)$$

In the equation,  $\mathbf{a}$  is the slope of the line and  $\mathbf{t}$  is the time vector for the period of time. In order to find  $\mathbf{x}$  estimates that minimize the cost function, the derivative of this function is taken, and the result is equated to zero. In this case, minimization of the cost function is turned into the solution of a system of equations as in Equation (15).

$$\mathbf{A}(\mu, \mathbf{k}_c) \begin{bmatrix} \mathbf{x} \\ \mathbf{a} \end{bmatrix} = \mathbf{b} \quad (15)$$

The matrix  $\mathbf{A}$  in Equation (16) and the vector  $\mathbf{b}$  in Equation (17) are calculated as,



171

$$172 \quad \mathbf{A}(\mu, k_c) = \begin{bmatrix} \sum_{m=1}^M \mathbf{W}_m + \mu \mathbf{H}(k_c) & -\mu \mathbf{H}(k_c) \\ \mathbf{t}^T \mathbf{H}(k_c) & -\mathbf{t}^T \mathbf{H}(k_c) \mathbf{t} \end{bmatrix} \quad (16)$$

173

$$174 \quad \mathbf{b} = \begin{bmatrix} \sum_{m=1}^M \mathbf{W}_m \mathbf{x}_m \\ 0 \end{bmatrix} \quad (17)$$

175

176 Using the equations above, the  $\tilde{\mathbf{x}}$  values showing the  $\mathbf{x}$  estimates are calculated as in Equation  
 177 (18).

178

$$179 \quad \begin{bmatrix} \tilde{\mathbf{x}}(\mu, k_c) \\ a \end{bmatrix} = \mathbf{A}^{-1}(\mu, k_c) \mathbf{b} \quad (18)$$

180

181 As a result, the proposed regularization method may be applied for both day-long and limited  
 182 periods of time (Arıkan et al. 2004).

183

## 184 **2.2 Global Ionosphere Model (GIM):**

185

186 Global Ionospheric Maps are published in the IONEX (IONosphere map EXchange) format in  
 187 a way that covers the entire world. The institutions that produce these maps in the world include  
 188 CODE (Center for Orbit Determination in Europe, Switzerland), DLR (FERNERKUNDUNGSTATION  
 189 Neustrelitz, Germany), ESOC (European Space Operations Centre, Germany), JPL (Jet  
 190 Propulsion Laboratory, California), NOAA (National Oceanic and Atmospheric  
 191 Administration, United States), NRCAN (National Resources, Canada), ROB (Royal  
 192 Observatory of Belgium, Belgium), UNB (University of New Brunswick, Canada), UPC  
 193 (Polytechnic University of Catalonia, Spain), WUT (Warsaw University of Technology,  
 194 Poland) (Aysezen, 2008). In this study we used the GIM-TEC values produced by CODE in the  
 195 IONEX format. In the dates they were analyzed, the temporal resolution of the TEC values was  
 196 2 hours, while their positional resolution was  $2.5^\circ$  by latitude and  $5^\circ$  by longitude. In order to  
 197 calculate TEC values for a point whose latitude and longitude is known on the GIM-TEC maps  
 198 created by CODE using more than 300 GNSS receivers around the world, the 4 TEC values  
 199 that cover the point and the two-variable interpolation formula are given below (Schaer et al.  
 200 1998).

$$201 \quad E_{int}(\lambda_0 + p\Delta\lambda, \beta_0 + q\Delta\beta) = (1-p)(1-q)E_{0,0} + p(1-q)E_{1,0} + q(1-p)E_{0,1} + pqE_{1,1} \quad (19)$$



202  $p$  and  $q$ :  $0 \leq p, q < 1$ .  
 203  $\Delta\lambda$  and  $\Delta\beta$ : Longitude and Latitude differences grid widths,  
 204  $\lambda_0$  and  $\beta_0$ : Initial longitude and latitude values,  
 205  $E_{0,0}, E_{1,0}, E_{0,1}$  ve  $E_{1,1}$  : TEC values known in neighboring points,  
 206  $E_{int}$ : TEC value to be found.

207

### 208 3. ANALYSIS TO DETERMINE EARTHQUAKE-RELATED TEC CHANGES

209

210 In order to investigate earthquake-related TEC changes, the TEC values for the stations close  
 211 to the epicenters, HAKK, MALZ, OZAL and TVAN were procured using the IONOLAB-TEC  
 212 and GIM-TEC models. The correlation coefficient was obtained for the TEC values from both  
 213 models between the dates 13.10.2011 and 02.11.2011 for the stations above.



214

215

**Figure 3.** Analyzed Stations

216 Figure 3 shows the stations analyzed (represented by red triangles) and the epicenter of the  
 217 earthquake represented by blue star. For each station, the TEC values with the temporal  
 218 resolution of two hours obtained from both the IONOLAB-TEC and GIM-TEC models and the  
 219 correlation coefficient showing whether there is a linear relationship between two values were  
 220 calculated as below;

221

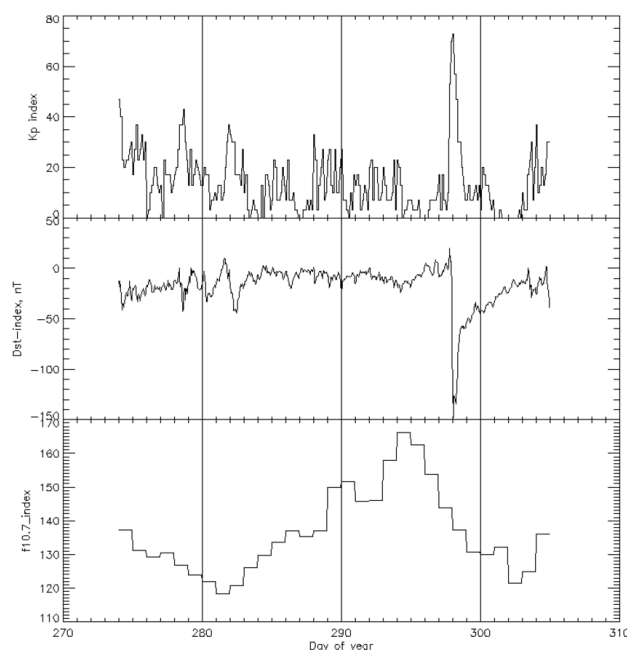
$$222 \quad r = \frac{\sum(xy) - (\sum x)(\sum y)/n}{\sqrt{(\sum x^2 - (\sum x)^2/n)(\sum y^2 - (\sum y)^2/n)}} \quad (20)$$





223

224 In order to determine the outlier values among the TEC values with a two-hour temporal  
 225 resolution from both models, the TEC values obtained from both models between the dates  
 226 01.10.2011 and 10.10.2011, which were considered calm in terms of geomagnetic and solar  
 227 activity, were used to determine the upper boundary (UB) and the lower boundary (LB). By  
 228 utilizing the TEC values from both models, the UB and LB values were calculated using the  
 229 formulae  $x+3\sigma$  and  $x-3\sigma$ . Here,  $x$  is the mean TEC value for the relevant epoch and  $\sigma$  is the  
 230 standard deviation. If the TEC value in any epoch is higher than the upper boundary, it is a  
 231 positive anomaly. Similarly if it is lower than the lower boundary, it is a negative anomaly. In  
 232 order to investigate whether the anomalies before, on the day of and after the earthquake were  
 233 caused by the earthquake or not, we also examined the Kp, Dst and F10.7 cm indices, which  
 234 provided information on the geomagnetic and solar activity for the days in which anomalies  
 235 were detected.

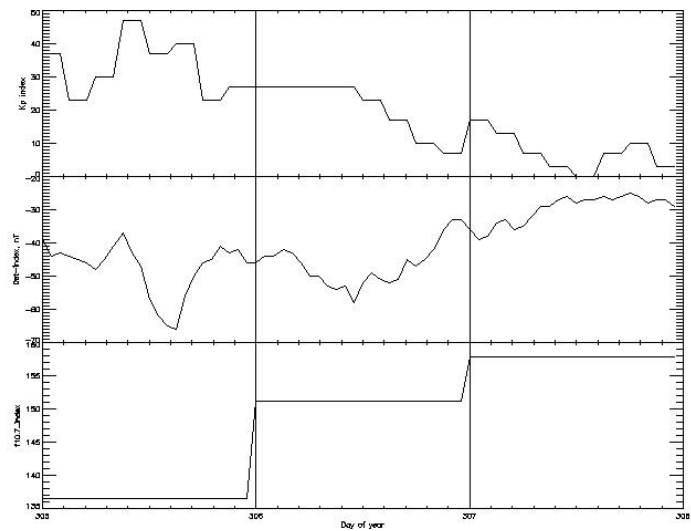


236

237

238

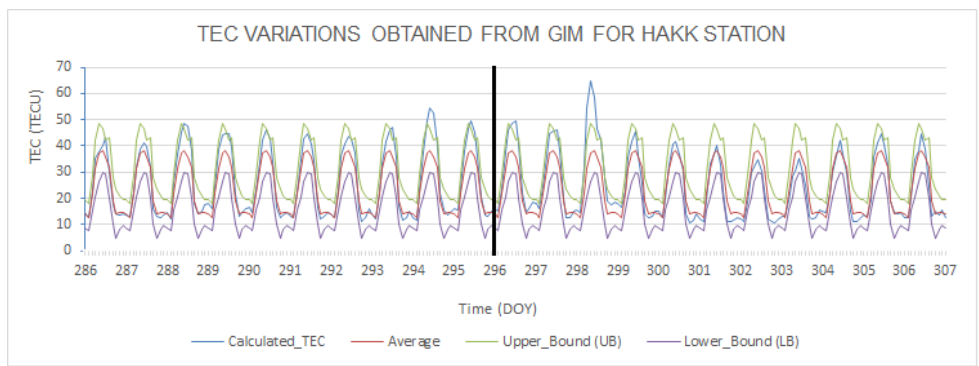
**Figure 4.** The Chart for October 2011 Kp, Dst and F10.7 cm Indices (URL-3)



239  
240 **Figure 5.** The Chart for the Dates 01-03.11.2011 in  $K_p$ , Dst and F10.7 cm Indices (URL-3)

241  
242 Figures 4 and 5 show the  $K_p$ , Dst and F10.7 cm indices that provide information on  
243 geomagnetic and solar activity in October and on the first three days of November. Below are  
244 the TEC values for the HAKK station for the dates 13.10.2011-02.11.2011 obtained using the  
245 GIM-TEC and IONOLAB-TEC methods (Figures 6 and 7).

246



247  
248 **Figure 6.** GIM-TEC Values for the HAKK Station

249

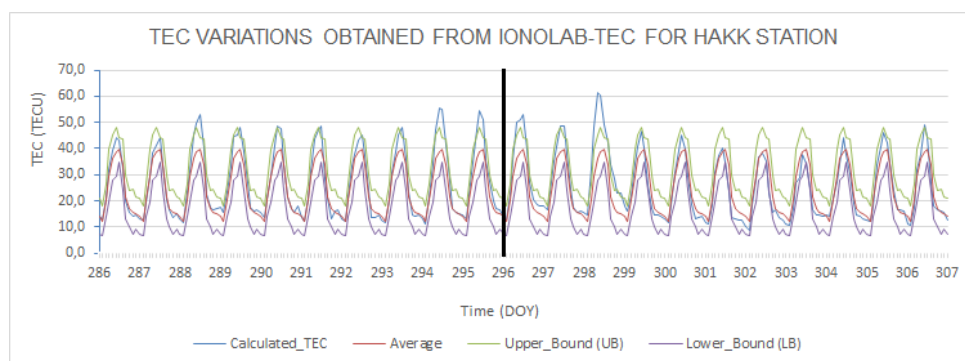


**Figure 7.** IONOLAB-TEC Values for the HAKK Station

The correlation coefficient  $r$  between the TEC values calculated by both methods for the HAKK station was 0.978469 indicating a strong positive relationship. The anomaly tables for this station are provided below (Tables 1 and 2).

GIM-TEC Anomaly Table for HAKK Station									
Number	DOY	Hour	TEC Difference (TECU)	Type of Anomaly	Number	DOY	Hour	TEC Difference (TECU)	Type of Anomaly
1	286	12	1.0	Positive	7	294	12	10.5	Positive
2	288	12	5.7	Positive	8	295	12	7.3	Positive
3	289	12	2.5	Positive	9	296	12	7.5	Positive
4	290	12	0.5	Positive	10	297	12	4.1	Positive
5	292	12	0.8	Positive	11	298	8	16.5	Positive
6	293	12	5.2	Positive					

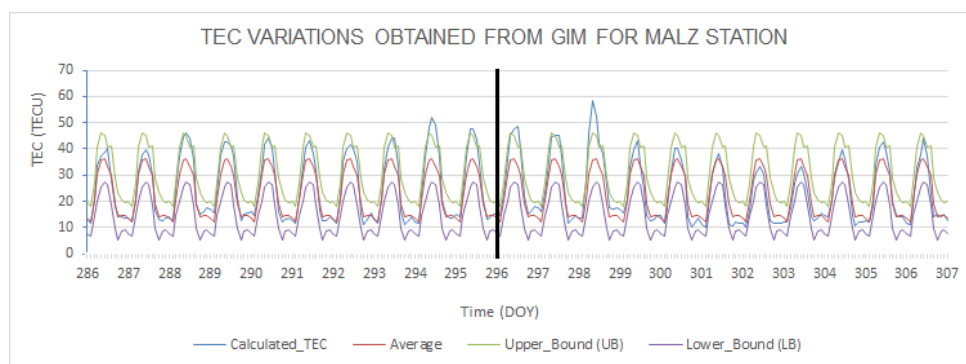
**Table 1.** HAKK Station Global Ionosphere Model Anomaly Table

IONOLAB-TEC Anomaly Table for HAKK Station									
Number	DOY	Hour	TEC Difference (TECU)	Type of Anomaly	Number	DOY	Hour	TEC Difference (TECU)	Type of Anomaly
1	287	12	0.4	Positive	9	295	12	7.2	Positive
2	288	12	9.2	Positive	10	296	12	8.8	Positive
3	289	12	4.3	Positive	11	297	12	4.6	Positive
4	290	12	3.8	Positive	12	298	8	16.5	Positive
5	291	12	4.5	Positive	13	301	12	0.3	Negative
6	292	12	1.4	Positive	14	302	14	0.9	Negative
7	293	12	4.2	Positive	15	303	12	0.7	Negative
8	294	12	10.9	Positive	16	306	10	0.9	Positive

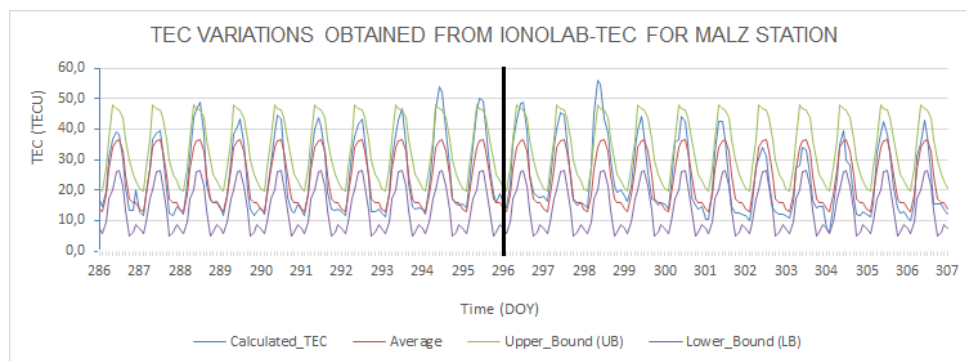
**Table 2.** HAKK Station IONOLAB-TEC Anomaly Table



260  
 261 Below are the TEC values for the MALZ station obtained using the GIM-TEC and IONOLAB-  
 262 TEC methods (Figures 8 and 9).  
 263



264  
 265 **Figure 8.** GIM-TEC Values for the MALZ Station



266  
 267 **Figure 9.** IONOLAB-TEC Values for the MALZ Station

268  
 269 The correlation coefficient  $r$  between the TEC values calculated by both methods for the MALZ  
 270 station was 0.976587 indicating also a strong positive relationship. The anomaly tables for this  
 271 station are provided below (Tables 3 and 4).  
 272

GIM-TEC Anomaly Table for MALZ Station									
Number	DOY	Hour	TEC Difference (TECU)	Type of Anomaly	Number	DOY	Hour	TEC Difference (TECU)	Type of Anomaly
1	288	12	3.5	Positive	5	295	12	3.1	Positive
2	289	12	0.5	Positive	6	296	12	7.9	Positive
3	293	12	3.9	Positive	7	297	12	4.7	Positive
4	294	12	8.6	Positive	8	298	8	12.6	Positive



**Table 3.** MALZ Station Global Ionosphere Model Anomaly Table

IONOLAB-TEC Anomaly Table for MALZ Station									
Number	DOY	Hour	TEC Difference (TECU)	Type of Anomaly	Number	DOY	Hour	TEC Difference (TECU)	Type of Anomaly
1	288	12	2.3	Positive	5	296	12	2.5	Positive
2	293	12	0.4	Positive	6	298	6	8.6	Positive
3	294	10	7.4	Positive	7	304	0	0.2	Negative
4	295	10	3.6	Positive					

**Table 4.** MALZ Station IONOLAB-TEC Anomaly Table

Tables 3 and 4 show the anomalies found as a result of the analysis of the TEC values obtained by the IONOLAB-TEC and GIM-TEC methods for the MALZ station. It is believed that the positive anomaly on days 288 and 289 was caused by moderate (136.9 sfu, 150 sfu) solar activity. It is also believed that the anomalies on the days 293, 294, 295 and 296 were caused by strong (157.8 sfu, 166.3 sfu, 162.5 sfu, 153.9 sfu) solar activity.

Below are the TEC values for the OZAL station obtained using the GIM-TEC and IONOLAB-TEC methods for the dates 13 October – 02 November (Figures 10 and 11).

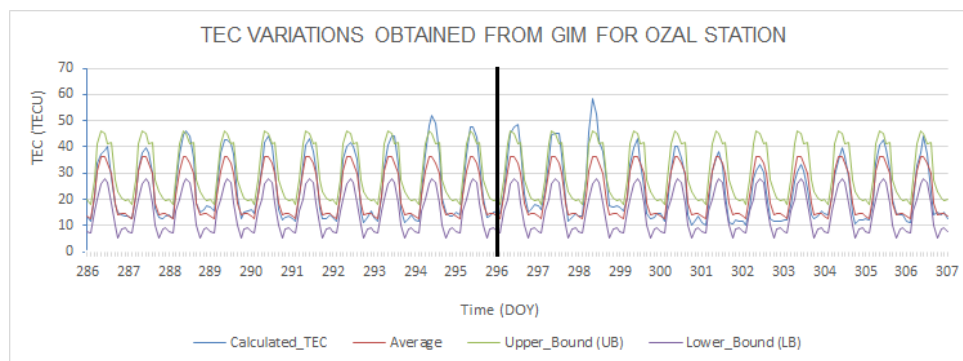


**Figure 10.** GIM-TEC Values for the OZAL Station

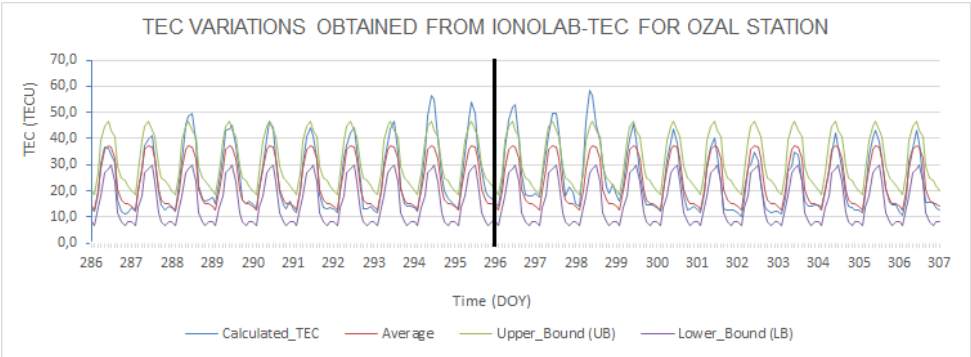


**Figure 11.** IONOLAB-TEC Values for the OZAL Station

The correlation coefficient  $r$  between the TEC values calculated by both methods for the OZAL station was 0.982774 demonstrating a strong positive relationship. The anomaly tables for this station are provided below (Tables 5 and 6).

GIM-TEC Anomaly Table for OZAL Station									
Number	DOY	Hour	TEC Difference (TECU)	Type of Anomaly	Number	DOY	Hour	TEC Difference (TECU)	Type of Anomaly
1	288	12	2.8	Positive	5	296	12	7.2	Positive
2	293	12	3.2	Positive	6	297	12	4.0	Positive
3	294	12	7.9	Positive	7	298	8	12.4	Positive
4	295	12	2.4	Positive					

**Table 5.** OZAL Station Global Ionosphere Model Anomaly Table

IONOLAB-TEC Anomaly Table for OZAL Station									
Number	DOY	Hour	TEC Difference (TECU)	Type of Anomaly	Number	DOY	Hour	TEC Difference (TECU)	Type of Anomaly
1	288	12	6.1	Positive	7	295	10	7.4	Positive
2	289	12	1.6	Positive	8	296	12	9.6	Positive
3	290	12	0.9	Positive	9	297	12	6.0	Positive
4	293	12	3.5	Positive	10	298	8	13.6	Positive
5	292	12	0.6	Positive	11	301	14	1.2	Negative
6	294	12	11.8	Positive	12	302	14	1.4	Negative

**Table 6.** OZAL Station IONOLAB-TEC Anomaly Table



Below are the TEC values for the TVAN station obtained using the GIM-TEC and IONOLAB-TEC methods (Figures 12, 13).

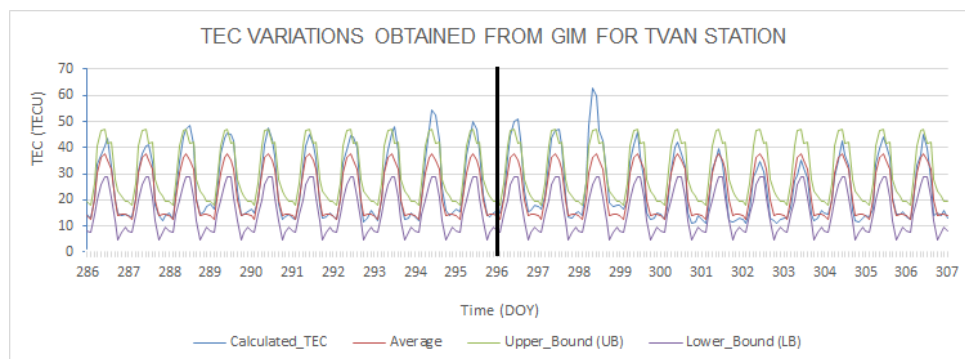


**Figure 12.** GIM-TEC Values for the TVAN Station

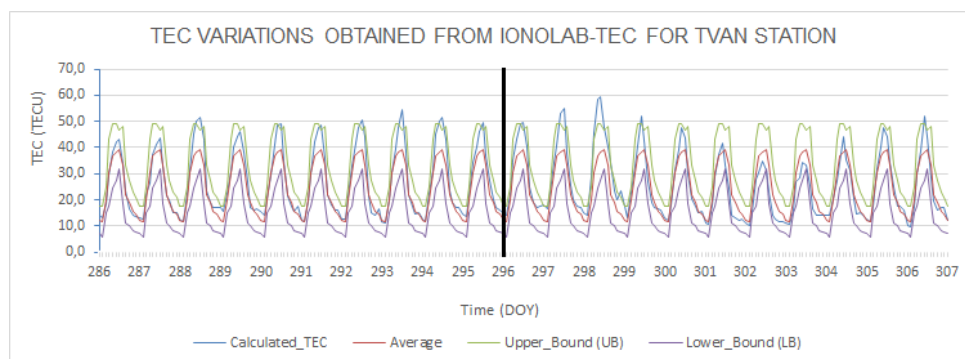


**Figure 13.** IONOLAB-TEC Values for the TVAN Station

The correlation coefficient between the TEC values calculated by both methods for the TVAN station was 0.978363 representing a strong positive relationship. The anomaly tables for this station are provided below (Tables 7 and 8).

GIM-TEC Anomaly Table for TVAN Station									
Number	DOY	Hour	TEC Difference (TECU)	Type of Anomaly	Number	DOY	Hour	TEC Difference (TECU)	Type of Anomaly
1	286	12	2.1	Positive	10	294	12	11.0	Positive
2	288	12	7.0	Positive	11	295	12	5.4	Positive
3	289	12	3.5	Positive	12	296	12	9.3	Positive
4	290	12	1.8	Positive	13	297	12	5.5	Positive
5	292	12	2.8	Positive	14	298	8	16.5	Negative
6	293	12	6.4	Positive					



**Table 7.** TVAN Station Global Ionosphere Model Anomaly Table

IONOLAB-TEC Anomaly Table for TVAN Station									
Number	DOY	Hour	TEC Difference (TECU)	Type of Anomaly	Number	DOY	Hour	TEC Difference (TECU)	Type of Anomaly
1	288	12	5.1	Positive	10	296	12	3.4	Positive
2	290	12	2.6	Positive	11	297	12	8.5	Positive
3	291	12	2.0	Positive	12	298	10	10.5	Positive
4	292	12	4.0	Positive	13	299	10	2.8	Positive
5	293	12	8.1	Positive	14	302	12	0.7	Negative
6	294	12	5.1	Positive	15	306	10	2.9	Positive
7	295	12	3.2	Positive					

**Table 8.** TVAN Station IONOLAB-TEC Anomaly Table

Tables 1, 2, 3, 4, 5, 6, 7 and 8 show the results of the statistical analysis of the TEC values created by the IONOLAB-TEC and GIM-TEC methods. The tables also depict the day and hour in which anomalies were observed, and the quantity and type of the anomaly. The numbers of anomalies obtained in both models were very close to each other. The F10.7 cm index values between the days 286 and 292 were 136 sfu, 135.4 sfu, 136.9 sfu, 150 sfu, 151.6 sfu, 145.7 sfu, 146.1 sfu. The index values show that there was usually moderate solar activity. Therefore, the anomalies in question may be related to the earthquake or solar activity. The index values for the days 293, 294, 295 and 296 (the day of the earthquake) were 157.8 sfu, 166.3 sfu, 162.5 sfu and 153.9 sfu respectively. These values indicate strong solar activity. On the other hand, the ionosphere layer was highly calm in these days in terms of geomagnetic conditions. As there was strong solar activity, the numbers of anomalies were higher than the numbers in the days 286-292. Since solar activity was moderate in the day 297, the number of anomalies dropped. The solar activity on the day 298 was moderate, but there was strong geomagnetic activity (Dst -147 nt, Kp\*10=73). The reason for the high numbers of anomalies on day 298 in both models is believed to be due to geomagnetic activity. Considering the analyzed days in general, it may be seen that it is difficult to identify earthquake-related anomalies as the solar activity and geomagnetic conditions before and after the earthquake were not calm. Therefore, it is believed that the anomalies detected in the stations on days 293-296 may be related to the earthquake and/or solar activity, and the anomalies on days 297 and 298 may be related to the earthquake, solar activity and/or geomagnetic activity.





#### 4. CONCLUSION

In the scope of this study, the TEC values for the stations HAKK, MALZ, OZAL, TVAN were obtained using the GIM-TEC and IONOLAB-TEC methods. In the comparison of the obtained values, it was seen that there was high correlation between the TEC values obtained by the two models. In order to detect earthquake-related TEC changes better, the TEC values created from both models for the period of 13.10.2011-02.11.2011 were used as reference to determine the UB and LB values. As a result of the statistical test, anomalies were found in all analyzed stations for before, on the day of and after the earthquake. In order to understand whether the anomalies obtained in both models were earthquake-related, the ionospheric conditions, geomagnetic activity and solar activity on the analyzed days were examined using the Kp, Dst and F10.7 cm indices.

Consequently, it was determined that the positive anomalies observed on days 286-292 may be related to moderate solar activity and/or the earthquake, and the positive anomalies observed on days 293, 294, 295, 296 (day of the earthquake) may be related to strong solar activity and/or the earthquake. Moderate solar activity and strong geomagnetic activity were observed for day 298, so the numbers of anomalies in both models increased dramatically. This increase is considered to be related to geomagnetic activity. The anomaly on day 298 may be related to the earthquake, geomagnetic effects and/or solar activity. The finding that the ionospheric conditions were vibrant in the analyzed days makes it highly difficult to identify earthquake-related ionospheric changes. Therefore, interdisciplinary studies are needed to determine the earthquake-related part of the change in question.



370 **BIBLIOGRAPHY:**

- 371 **Anderson, D., & Fuller-Rowell, T. (1999).** The ionosphere. Boulder, CO (325 Broadway,  
372 Boulder 80303-3326): Space Environment Center  
373
- 374 **Arikan F, Erol C B and Arikan O (2003)** Regularized Estimation Of Vertical Total Electron  
375 Content From Global Positioning System Data, Journal of Geophysical Research. 118,  
376 1469-1480, 2003  
377
- 378 **Arikan F, Erol C B and Arikan O (2004)** Regularized Estimation of Vertical Total Electron  
379 Content from GPS Data for a Desired Time Period, Radio Science, 39:RS6012.,  
380
- 381 **Arikan F, Arikan O and Erol C B (2007)** Regularized estimation of TEC from GPS data for  
382 certain midlatitude stations ve comparison with IRI model Cospar, Advances In Space  
383 Research, ISSN: 0273-1177, Vol.39.  
384
- 385 **Aslan N (2004)** GPS ile İyonosfer Toplam Elektron Yoğunluğu Değişimlerinin Koordinatlara  
386 Etkisinin Araştırılması Doktora Tezi, Yıldız Teknik Üniversitesi, Fen Bilimleri  
387 Enstitüsü.  
388
- 389 **Ayşezen M S (2008)** Türkiye için IONOLAB-TEC Kullanılarak GPS Tabanlı TEM ve Alıcı  
390 Yanıtlığı Veri Tabanı Hazırlanması, Yüksek Lisans Tezi, Zonguldak Karaelmas  
391 Üniversitesi.  
392
- 393 **Başpınar S (2012)** CORS-TR Verileriyle İyonosfer Modellerinin İncelenmesi, Doktora Tezi,  
394 İstanbul Ticaret Üniversitesi, Fen Bilimleri Enstitüsü.  
395
- 396 **Barnes R A and Leonard R S (1965)** Observations of ionospheric disturbances following the  
397 Alaska earthquake. J GeophysRes70: 1 250–1 253.  
398
- 399 **Erol C.B., Arikan F., (2004),** “GPS Sinyalleri ile İyonosferin İstatistiksel Özelliklerinin  
400 Belirlenmesi”, URSI-Türkiye., İkinci Ulusal Kongresi, 2004.  
401
- 402 **Erol C.B., Arikan F., (2005),** “Statistical Characterization of the Ionosphere Using GPS  
403 Signals”, J. of Electromagnetic Waves an Appl., Vol.19, No:3, 2005.



- 404  
405 **Gümrükçü O (2009)** GPS Sinyalleri İle Konum Belirlemede İyonosferik Etkilerin İncelenmesi  
406 Yüksek Lisans Tezi, Yıldız Teknik Üniversitesi, Fen Bilimleri Enstitüsü.  
407  
408 **İnyurt S (2015)** İyonosferdeki Toplam Elektron Miktarı (Tec) Ve Kod Yanlılık Değerlerinin  
409 (DCB) GNSS Ölçümleriyle Belirlenmesi Yüksek Lisans Tezi, Bülent Ecevit  
410 Üniversitesi, Fen Bilimleri Enstitüsü.  
411  
412 **Langley R B (2002)** Monitoring the Ionosphere and Neutral Atmosphere with GPS Division  
413 of Atmospheric and Space Physics Workshop, Fredericton, N.B., 21-23 February  
414 2002.  
415  
416 **Mekik Ç (1999)** GPS' e Atmosferin Etkileri, TMMOB Harita ve Kadastro Mühendisleri Odası  
417 Dergisi, Sayı: 86.  
418  
419 **Pulinets S. A. (1998)**, "Strong earthquakes prediction possibility with the help of top side  
420 sounding from satellites". Advances in Space Research 21(3): 455–458.  
421  
422 **Schaer S (1999)** Mapping and Predicting the Earth's Ionosphere Using the Global Positioning  
423 System, Doktora Tezi, University of Bern, İsviçre.  
424  
425 **Schaer, S., W. Gurtner, and J. Feltens, IONEX:** The IONosphere Map EXchange format  
426 Version 1, in Proceedings of the IGS Analysis Center Workshop, edited by J. M. Dow,  
427 J. Kouba, and T. Springer, Darmstadt, February 9 – 11, 1998.  
428  
429 **Ünver O (2010)** İyonosferik Toplam Elektron İçeriği (TEC) Değişiminin Belirlenmesi Yüksek  
430 Lisans Tezi, Yıldız Teknik Üniversitesi, Fen Bilimleri Enstitüsü.  
431 **Yildirim, O., Inyurt, S., Mekik, C. (2016).** Review of variations in  $M_w < 7$  earthquake  
432 motions on position and TEC ( $M_w = 6.5$  Aegean Sea earthquake sample). *Natural*  
433 *Hazards and Earth System Sciences*, 16(2), 543-557.  
434  
435 URL-1 [www.ionolab.org.tr](http://www.ionolab.org.tr)  
436 URL-2 <https://tr.wikipedia.org/wiki/iyonosfer>  
437 URL-3 <https://omniweb.gsfc.nasa.gov/form/dx1.html>